Synthesis and characterization of porous maghemite as an anode for Li-ion batteries

M. Golmohammad[a,b], F. Golestanifard[a,*], A. Mirhabibi[a,c], E.M. Kelder[b]

[a]School of Metallurgy and Materials Engineering, Iran University of Science and Technology (IUST), Tehran, Iran
[b]Faculty of Applied Sciences, Delft University of Technology, Delft, Netherlands
[c]Institute for Materials Research, University of Leeds, Leeds, United Kingdom

Abstract

The synthesis of porous maghemite via a simple glycerol-mediated solution method was successfully accomplished. Thermal analysis, X-ray diffraction and Mössbauer spectroscopy results disclosed the formation of maghemite. The morphological and structural features of maghemite were characterized by scanning electron microscopy, high-resolution transmission electron microscopy, and nitrogen adsorption–desorption. The powder showed Brunauer–Emmett–Teller surface area of 285 $m^2 g^{-1}$ with micro-, meso- and macropores.

The anode body was doctor bladed using primary powder with a binder and a conductive agent. Galvanostatic charge–discharge cycling of the porous maghemite exhibited a specific reversible capacity of approximately 1180 mAh g^{-1} at 100 mA g^{-1} current density, which was two times higher than that of common nanomaghemite with average particle size of 19 nm. The cell showed stability even at the high current charge–discharge rates of 3000 mA g^{-1} and more than 94% retention. After multiple high current cycling regimes, the cell recovered to nearly full reversible capacity of $\sim$1120 mAh g^{-1} at 100 mA g^{-1}. The reason for this remarkable performance of the present anode was thought to be dependent upon the role of pores in increasing the surface area and resistance against volume changes during lithium insertion/extraction.
© 2015 Elsevier Ltd and Techna Group S.r.l. All rights reserved.

Keywords: Maghemite; Porous; Li-ion battery; Anode; Capacity retention

1. Introduction

The high energy and power density of Li-ion batteries make them the first choice for portable electronics, power tools, and electric vehicles [1]. One of the main hurdles for improving Li-ion battery performance is the electrode material employed [2,3]. The electrode material should be inexpensive and nontoxic and demonstrate high capacity and stability as an electrode [1,4]. Iron oxide was first introduced as an electrode material candidate by Poizot et al. [5]. Since then, iron oxides have attracted much attention in Li-ion battery electrodes [6–14] because of their high capacity, low price and availability of material. The reversible conversion reaction between lithium ions (Li^+) and iron oxides (Fe_xO_y) is the main reason for the high capacity of iron oxides, as shown by Eq. (1).

$$Fe_xO_y + 2yLi^+ + 2ye^- \leftrightarrow xFe + yLi_2O \tag{1}$$
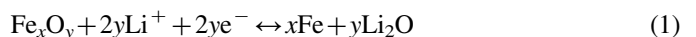
Different types of iron oxides such as (α-Fe_2O_3) [6–8,13], magnetite (Fe_3O_4) [9–11] and maghemite (γ-Fe_2O_3) [12,14] have been investigated as battery electrodes. However, the main bottlenecks are low initial coulombic efficiency and capacity fading during charge–discharge which are due to the low electrical conductivity and drastic volume change during the charge–discharge process. One potential solution to the latter hurdle is to use porous powder that can release some of volume changes during charge and discharge. Moreover, porosity will increase the surface area and effectively prepare more surface for the Li and metal oxide reaction.

*Corresponding author. Tel./fax: +98 21 77 240 291.
E-mail address: Golestanifard@iust.ac.ir (F. Golestanifard).

Different methods have been introduced for the synthesis of iron oxide such as hydrothermal methods [15,16], microemulsion [17,18], co-precipitation [12,19,20], solution methods [21,22], thermal decomposition [23–25] and microwave synthesis [26]. Mediated solution methods without any surfactant have recently been proved to be a promising synthesis route for preparing monodisperse porous particles [21–23]. Jia et al. [21] synthesized lepidocrocite using ethylene glycol with a simple mediated solution method. Moreover, Asuha et al. [23] prepared mesoporous magnetite with an average pore size of 3.6 nm using triethylene glycol (TEG) as a polyol solvent. One of other soluble polyols in water is glycerol which binds precipitated particles that in subsequent steps can produce porosity [27]. To our knowledge, there has been no report on the properties of porous maghemite as an anode in Li-ion batteries. Additionally, most of the preparation methods for the synthesis of porous powders are complicated.

In this work, porous maghemite with high surface area was synthesized with a facile glycerol-mediated solution method that showed remarkable battery cycling properties. These porous particles delivered excellent specific reversible capacity of 1180 mAh g^{-1} at 100 mA g^{-1}, and preserved cycling at extremely high current density (3000 mA g^{-1}).

2. Experimental procedure

2.1. Materials and methods

In a typical synthesis process, 1 mol of iron (III) nitrate nonahydrate (Fe $(NO_3)_3 \cdot 9H_2O$, Sigma-Aldrich) was dissolved in a (50–50) mixture of deionized water and glycerol ($C_3H_8O_3$, Sigma-Aldrich) at room temperature. Then, 4 mol of urea (CH_4N_2O, Sigma-Aldrich) was added to the solution and stirred for 10 min. The solution was heated at 110 °C for 12 h in a conical flask with a stopper and allowed to cool to room temperature naturally. The resulting deep-brown sticky precipitates were collected by centrifugation and washed with deionized water repeatedly until a neutral pH was achieved. These sticky precipitates were heated at different temperatures to obtain maghemite. For comparison of battery cycling properties, the C5 sample (dense maghemite nanopowders with 19 nm particle size and 60 $m^2 g^{-1}$ surface area) was synthesized with the co-precipitation method, the details of whose preparation are described elsewhere [12].

For preparation of the electrode, optimized powder was milled and mixed with graphite/acetylene black (50–50) and polyvinylidene difluoride powder (PVdF, Solef) at a weight ratio of 8:3:2 using N-methyl pyrrolidone (NMP, Merk-Schuchardt) as dissolving solvent. The mixture was doctor bladed on an etched copper foil as a current collector up to a thickness of 100 μm. The copper foil was then dried at 110 °C, and circular disks (14 mm in diameter) were punched out, which then served as the test electrodes. Metallic lithium disks were used as reference and counter electrodes and 1 M LiPF6 dissolved in ethylene carbonate (EC) and dimethyl carbonate (DMC) (2:1 by wt, Mitsubishi Chemicals) was used as the electrolyte. These electrodes were stacked together in a CR2320 coin cell (Hohsen) assembled in an Ar-filled glovebox (MBraun).

2.2. Characterization

Simultaneous thermal analysis (STA) was conducted with an STA Instruments 2960 device. Powder X-ray diffraction (XRD) measurements were carried out with Bruker device (AXS D8 Advance) using Co-K$_\alpha$ radiation. The iron state has been detected by Mössbauer spectroscopy using a Mössbauer SM 1201 spectrometer at room temperature with a ^{57}Co/Rh source in a constant acceleration transmission spectroscopy. The spectrometer was calibrated using a standard α-Fe foil and the reported isomer shifts are relative to the center of the α-Fe spectrum. The microstructure and morphology of the samples were recorded using a scanning electron microscope (SEM, JEOL JSM- 6700F), a field-emission scanning electron microscope (FESEM, TSCAN-Mira3), and a high-resolution transmission electron microscope (HR-TEM, Philips EM201C). A nitrogen adsorption–desorption test was carried out with a Micrometer device.

Galvanostatic tests were performed with a Maccor cycler (S-4000) and the cycling performance and capacity were monitored. Before the electrochemical measurements, the cells were aged for 12 h. The voltage limits were set to 0.01 and 3 V vs. Li/Li$^+$.

3. Results and discussion

3.1. Characterization of synthesized powder

The STA pattern for the sticky precipitates is presented in Fig. 1. The thermogravimetric analysis curve shows four distinct transitions between room temperatures and 700 °C with a total weight loss of 72%. The first weight loss was 12%, which started from 80 °C and continued until approximately 180 °C. This weight loss was in accordance with an endothermic peak in the differential thermal analysis (DTA), which is due to the evaporation of absorbed water and trapped water-glycerol. The second weight loss was 31% between 180 and
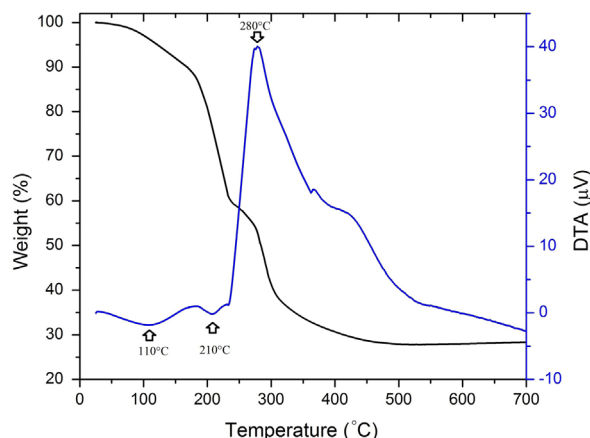

Fig. 1. STA result of as-synthesized powder sample.